Heavy Quark Spectroscopy Results from LHCb

Charlotte Wallace
on behalf of the LHCb collaboration
Lake Louise Winter Institute 2015
19th February 2015

European Research Council
Established by the European Commission

Introduction and overview

- **New results** on D^{**} states from $B^- \to D^+K^-\pi^-$
  - First observation of decay mode
  - Resonant structure studied with a Dalitz plot analysis
  - Observed spin-1 resonance $D_1^*(2760)$

LHCb-PAPER-2015-007
to be submitted to PRD

- **New results** on B^{**} states in $B^+\pi^-$ and $B^0\pi^+$ spectra
  - Low mass states precisely measured
  - Structures observed at higher mass
  - $B_2^*(5747)$ and $B_1(5721)$ states observed

arXiv:1502.02638
submitted to JHEP

D^{**} Spectroscopy with $B^- \to D^+K^-\pi^-$

- Dalitz plot analysis is a powerful tool
  - Previously used by B-factories to study charm spectroscopy
  - Used at LHCb for D_s spectroscopy ($B_s^0 \to \overline{D}^0 K^- \pi^+$) [Phys. Rev. D90 (2014) 072003, Phys. Rev. Lett. 113 (2014) 162001]
  - Clean and constrained method compared to inclusive production studies
  - Allows determination of quantum numbers for states

- $B^- \to D^+K^-\pi^-$ is an interesting mode to study D^{**} states
  - Decay previously unobserved, first measure branching fraction
  - No resonances expected to decay to D^+K^- or $K^-\pi^-$

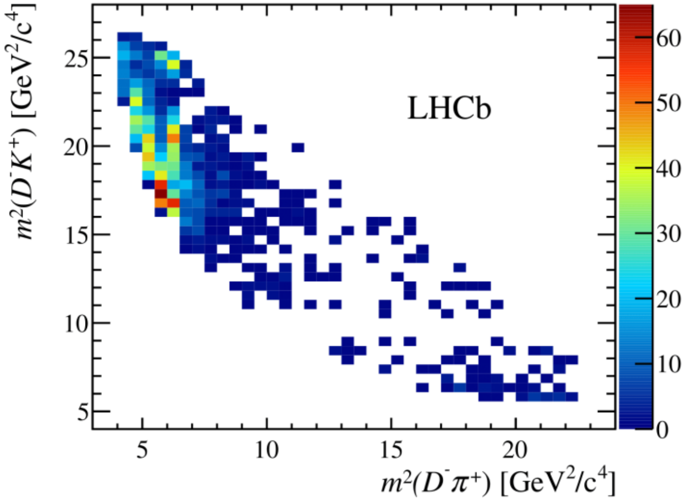

- Use Laura++ Dalitz plot fitting software
  - Available on Hepforge

Dalitz plot of $B^- \to D^+ K^- \pi^-$

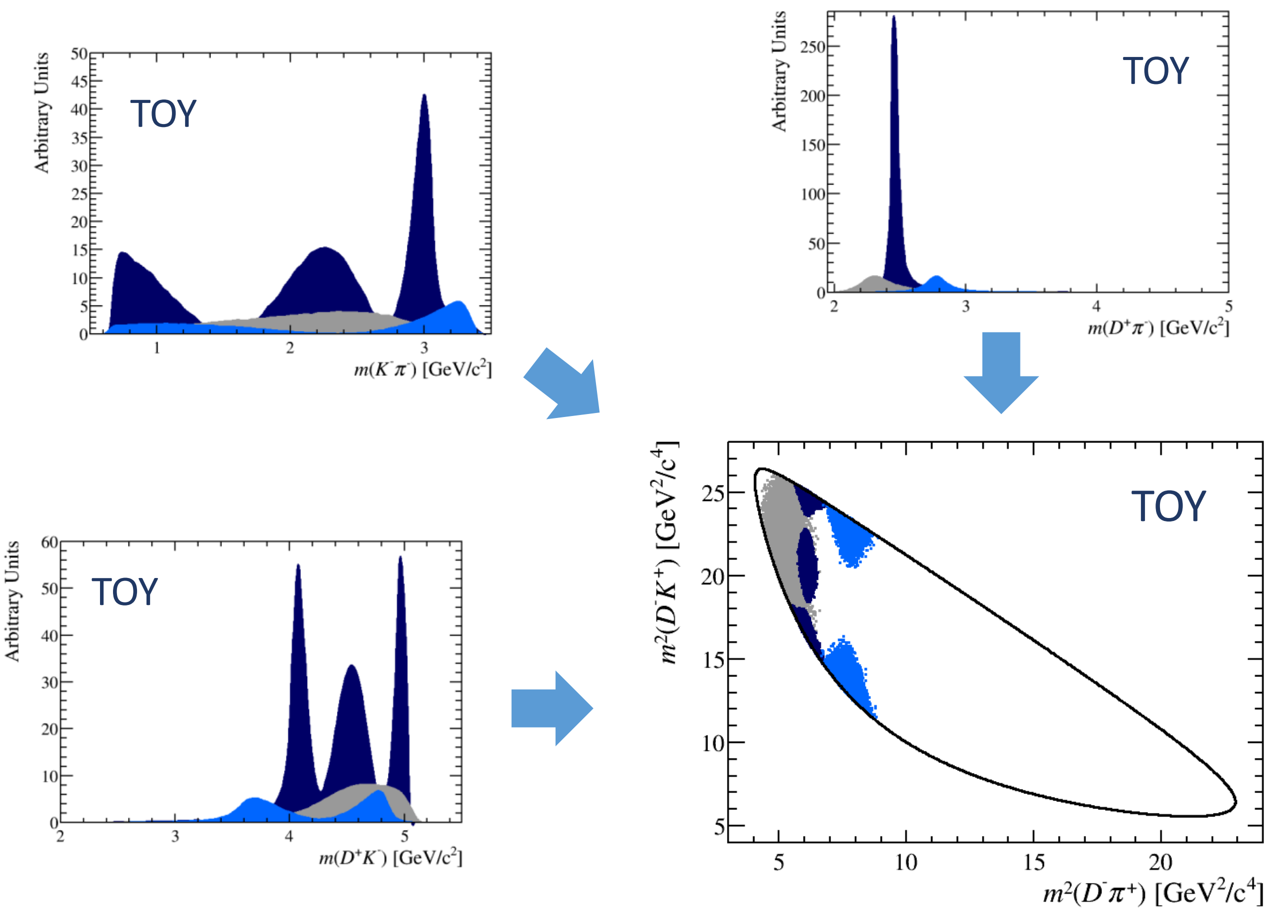

- See resonant structures in invariant mass of pairs of daughters
- Reflections visible in other invariant mass pairs
- 2D representation is "Dalitz plot"
- Interference effects visible

D^{**} Spectroscopy

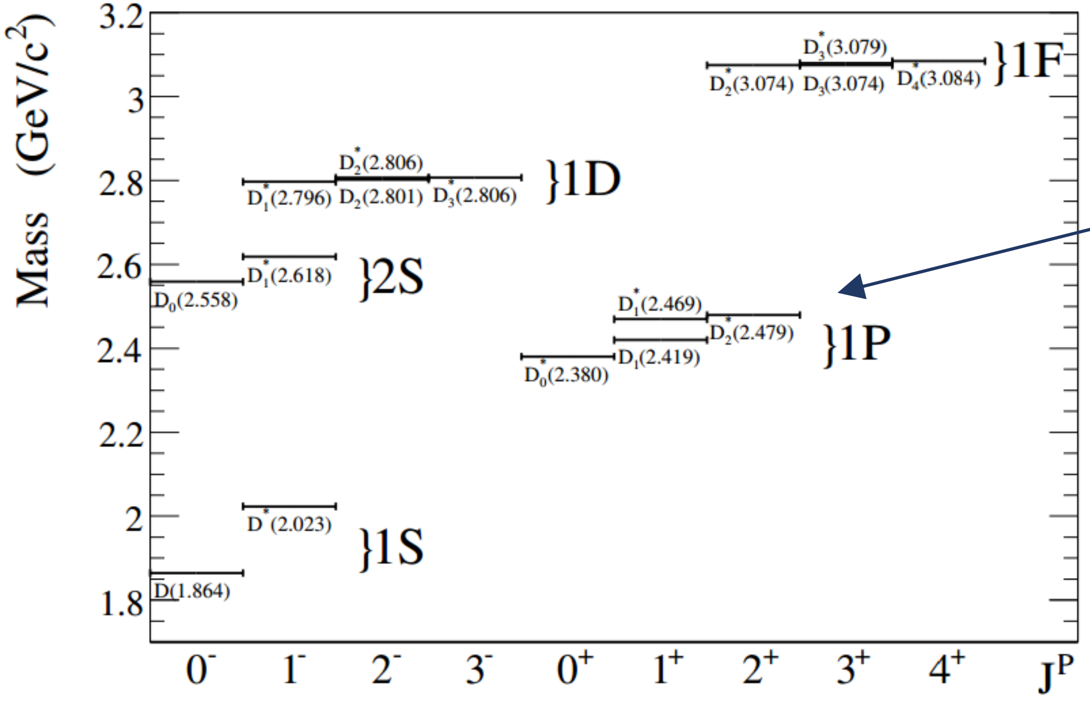

Parameters of orbitally excited (1P) states measured at B-factories and LHCb

Phys. Rev. D69 (2004) 112002
Phys. Rev. D79 (2009) 112004
Phys. Rev. D82 (2010) 111101
JHEP 1309 (2013) 145

- Charm spectrum predicted [S. Godfrey, N. Isgur, Phys. Rev. D32 (1985) 189]
- Experimental results come from Dalitz plot analyses and prompt production
- Some discrepancies between predicted and measured values
- Evidence for higher mass states, but not yet possible to assign quantum numbers

D^{**} Spectroscopy with $B^- \to D^+ K^- \pi^-$

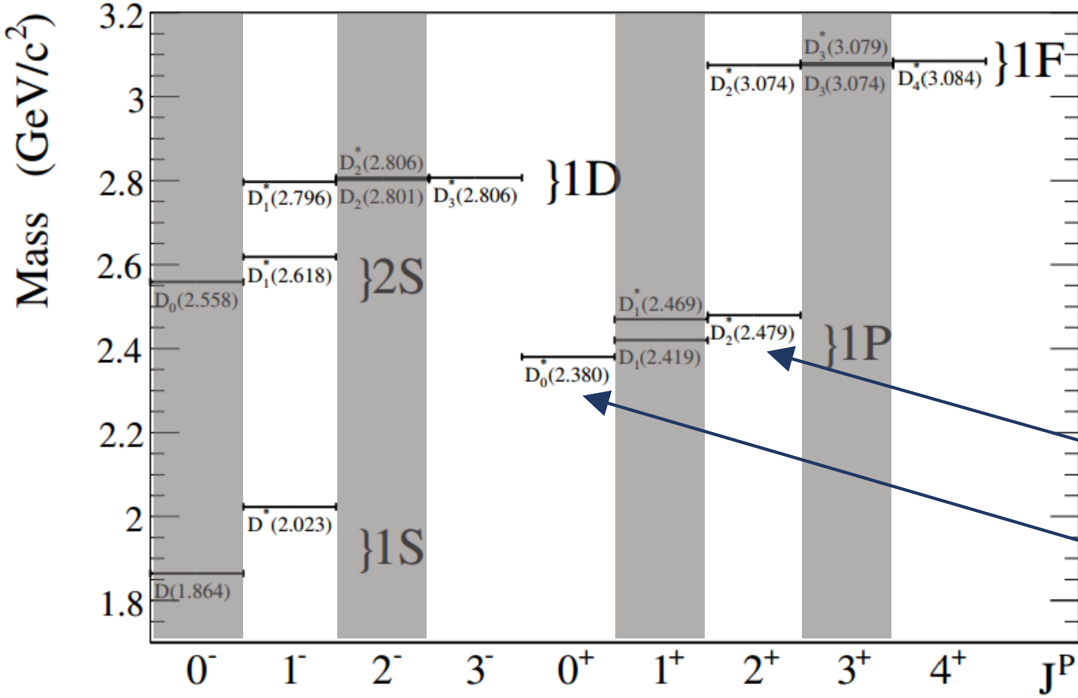

Evidence for several high mass states but no spin-parity information yet

$D_2^*(2460)^0$

$D_0^*(2400)^0$

- Spectrum can be studied with a Dalitz plot analysis of $B^- \to D^+ K^- \pi^-$
- Only states with **natural spin-parity** (J^P) can decay to $D^+\pi^-$
- $D_0^*(2400)^0$, $D_2^*(2460)^0$ and higher mass states expected to contribute
- Amplitude analysis techniques give spin-parity information

Branching fraction measurement

- Events selected with loose cuts and neural network used to reduce backgrounds
  - [M. Feindt and U.Kerzel, Nucl. Instrum. Meth. A559 (2006) 190]

- ~2000 $B^- \to D^+K^-\pi^-$ candidate events (> 60σ observation!)

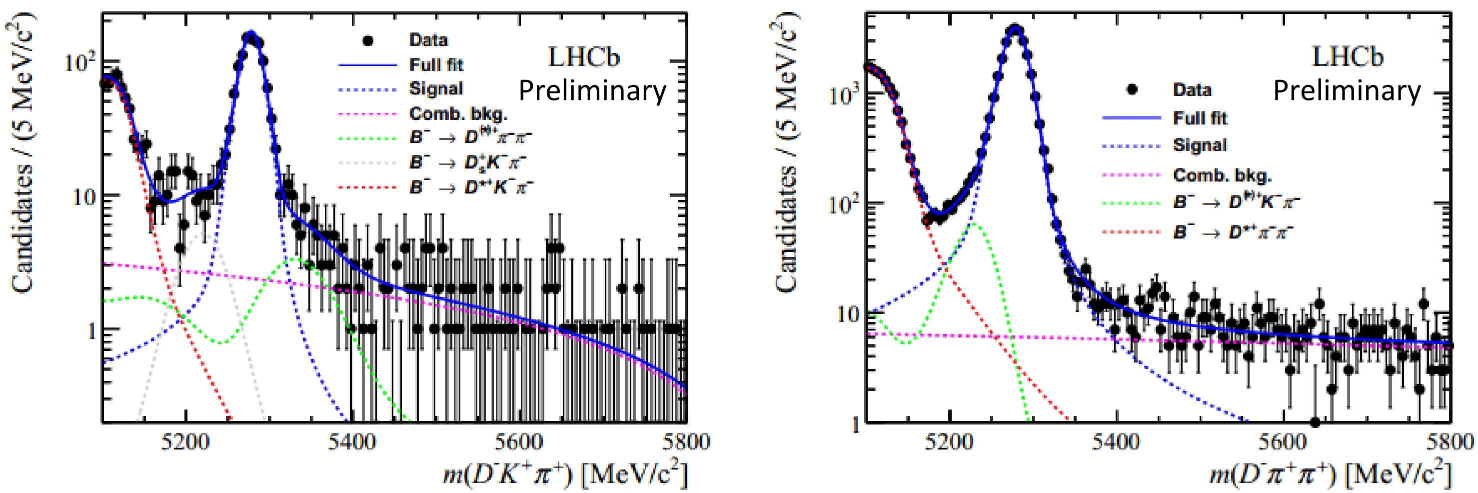

- Branching fraction measured wrt to $B^- \to D^+\pi^-\pi^-$

$$\mathcal{B}(B^- \to D^+K^-\pi^-) = (7.92 \pm 0.23 \pm 0.24 \pm 0.42) \times 10^{-5}$$

Uncertainties are statistical, systematic and due to PDG uncertainty on $B^- \to D^+\pi^-\pi^-$ BF

Dalitz plot model

- Efficiency and background distributions studied and used as input

Resonance	Spin	DP axis	Model	Parameters
$D_0^*(2400)^0$	0	$m^2(D\pi)$	RBW	$m = 2318 \pm 29\,\text{MeV}/c^2,\ \Gamma = 267 \pm 40\,\text{MeV}$
$D_2^*(2460)^0$	2	$m^2(D\pi)$	RBW	Floated
$D_J^*(2760)^0$	1	$m^2(D\pi)$	RBW	Floated
Nonresonant	0	$m^2(D\pi)$	EFF	Floated
Nonresonant	1	$m^2(D\pi)$	EFF	Floated
$D_v^*(2007)^0$	1	$m^2(D\pi)$	RBW	$m = 2006.98 \pm 0.15\,\text{MeV}/c^2,\ \Gamma = 2.1\,\text{MeV}$
B_v^{*0}	1	$m^2(DK)$	RBW	$m = 5325.2 \pm 0.4\,\text{MeV}/c^2,\ \Gamma = 0.0\,\text{MeV}$

- $D_0^*(2400)^0$ and $D_2^*(2460)^0$ states expected
- High mass $D_J^*(2760)^0$ state included, previously unknown spin
- Two virtual states

- Relativistic Breit-Wigner shape used to model resonances

- Two non-resonant components (S-wave and P-wave), exponential model
  - Model independent tests support need for both

Dalitz plot fit

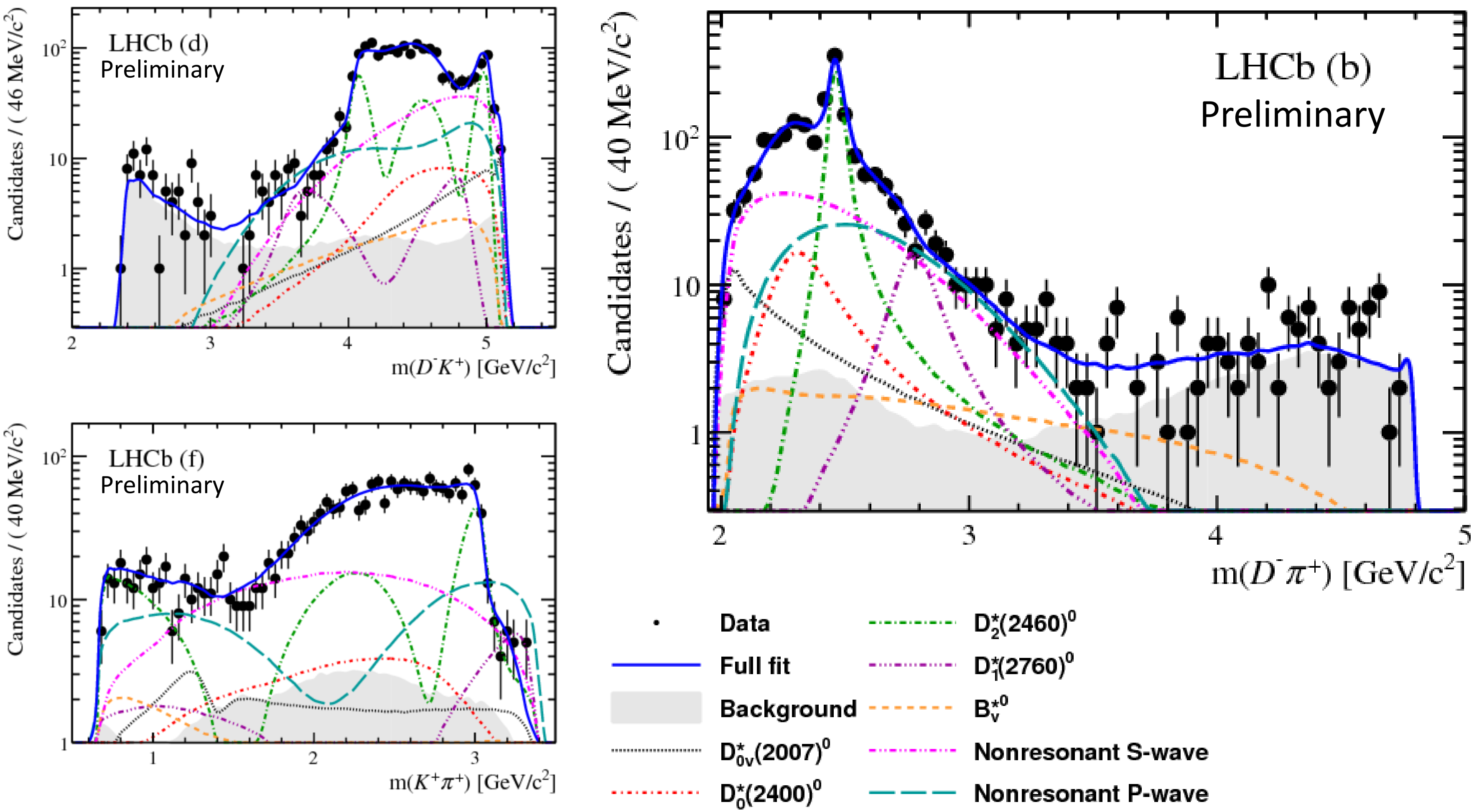

Dalitz plot fit

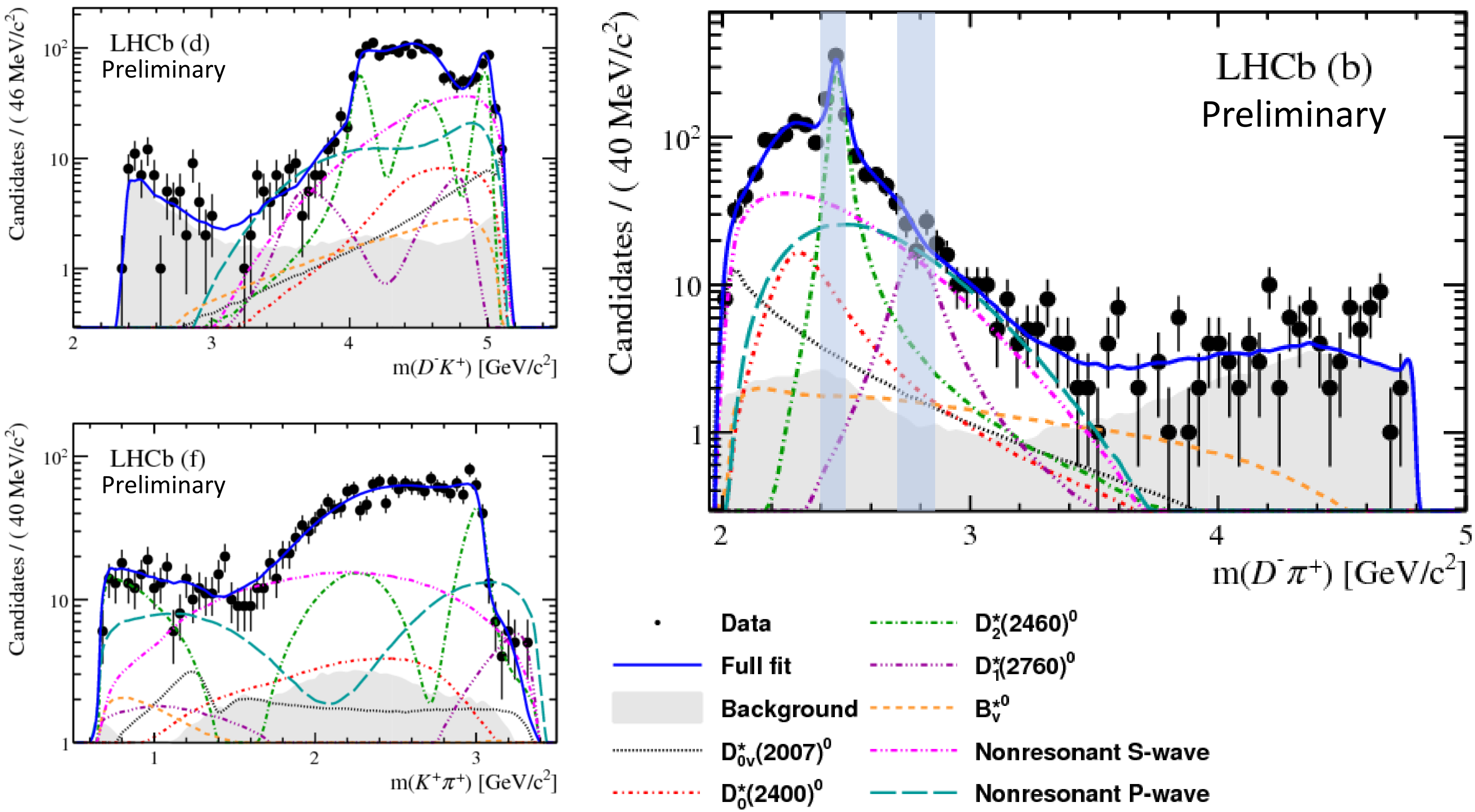

Dalitz plot fit

- (Right) helicity angle distributions for (left) interesting $m(D^{+}\pi^{-})$ regions

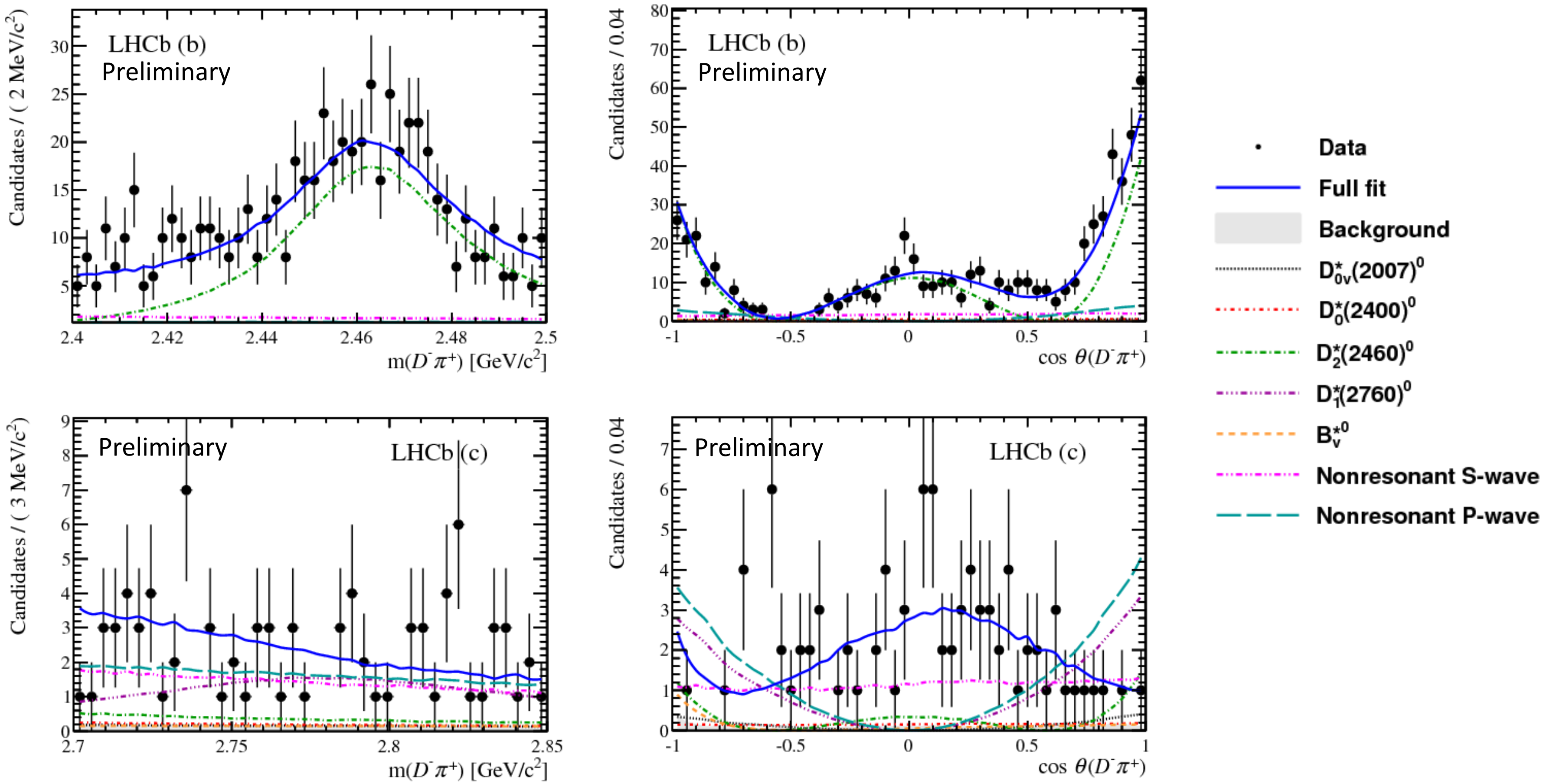

Dalitz plot analysis results

- $D_1^*(2760)^0$ determined to have spin-1
  - Other hypotheses rejected with high significance

- Masses and widths of $D_2^*(2460)^0$ and $D_1^*(2760)^0$ reported:

$$m(D_2^*(2460)^0) = (2464.0 \pm 1.4 \pm 0.5 \pm 0.2)\,\mathrm{MeV}/c^2$$
$$\Gamma(D_2^*(2460)^0) = (43.8 \pm 2.9 \pm 1.7 \pm 0.6)\,\mathrm{MeV}$$
$$m(D_1^*(2760)^0) = (2781 \pm 18 \pm 11 \pm 6)\,\mathrm{MeV}/c^2$$
$$\Gamma(D_1^*(2760)^0) = (177 \pm 32 \pm 20 \pm 7)\,\mathrm{MeV}$$

Uncertainties are statistical, experimental systematic and model uncertainties

- Product branching fractions ($\times\,10^{-4}$) measured:

Resonance	Branching fraction
$D_0^*(2400)^0$	$6.6 \pm 2.1 \pm 0.5 \pm 1.5 \pm 0.4$
$D_2^*(2460)^0$	$25.2 \pm 1.2 \pm 0.7 \pm 1.1 \pm 1.7$
$D_1^*(2760)^0$	$3.9 \pm 1.0 \pm 0.3 \pm 0.7 \pm 0.3$
S-wave nonresonant	$30.1 \pm 5.9 \pm 1.2 \pm 8.6 \pm 2.0$
P-wave nonresonant	$18.9 \pm 4.4 \pm 1.6 \pm 2.9 \pm 1.3$
$D_v^*(2007)^0$	$6.0 \pm 1.8 \pm 1.0 \pm 1.2 \pm 0.4$
B_v^*	$2.9 \pm 1.5 \pm 0.7 \pm 1.3 \pm 0.2$

Final errors due to uncertainty on $DK\pi$ BF result

B^{**} Spectroscopy

B^{**} Spectroscopy

- Heavy Quark Effective Theory predicts spectrum of excited B states
  - Spectrum should be almost identical for charged and neutral B^{**} states
  - Higher excitations decay to B/B^{*} plus π

- Current knowledge is limited

- Broad B_0^* and B_1 states predicted
- Narrow B_1 and B_2^* states observed by CDF and D0 [Phys. Rev. Lett. 102 (2009) 102003, Phys. Rev. Lett. 99 (2007) 172001]
- Evidence for higher mass states from CDF [Phys. Rev. D90 (2014) 012013]

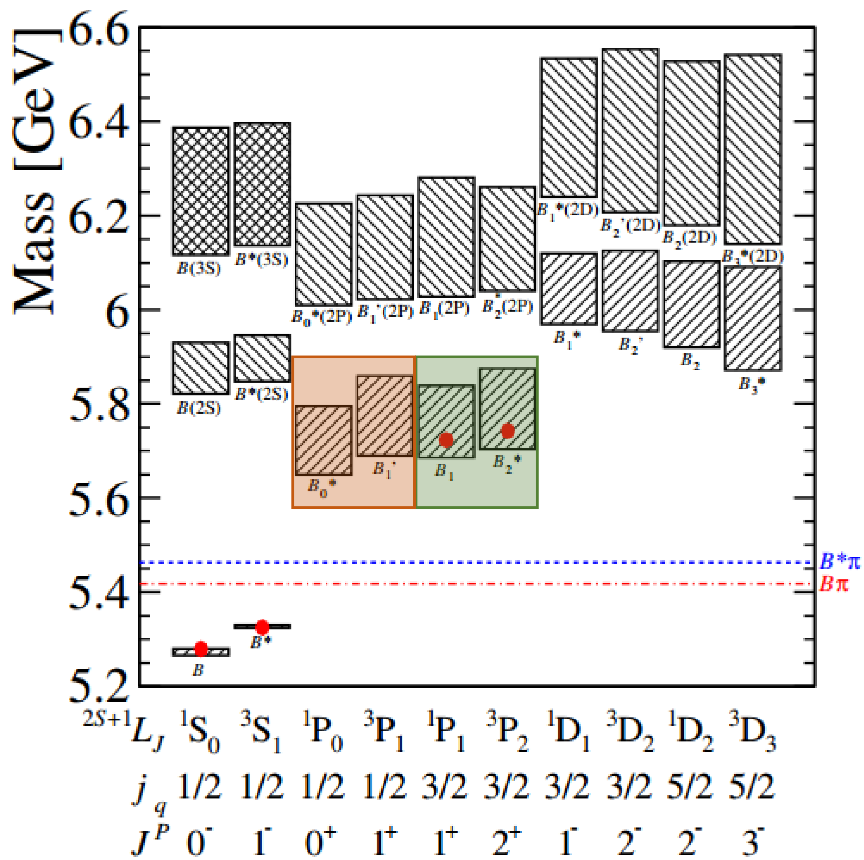

Fit to data

- Simultaneous fit to 3 bins for p_T of companion pion
  - Fit results shown for (left) $B^+\pi^-$ and (right) $B^0\pi^+$ (integrated over p_T bins)

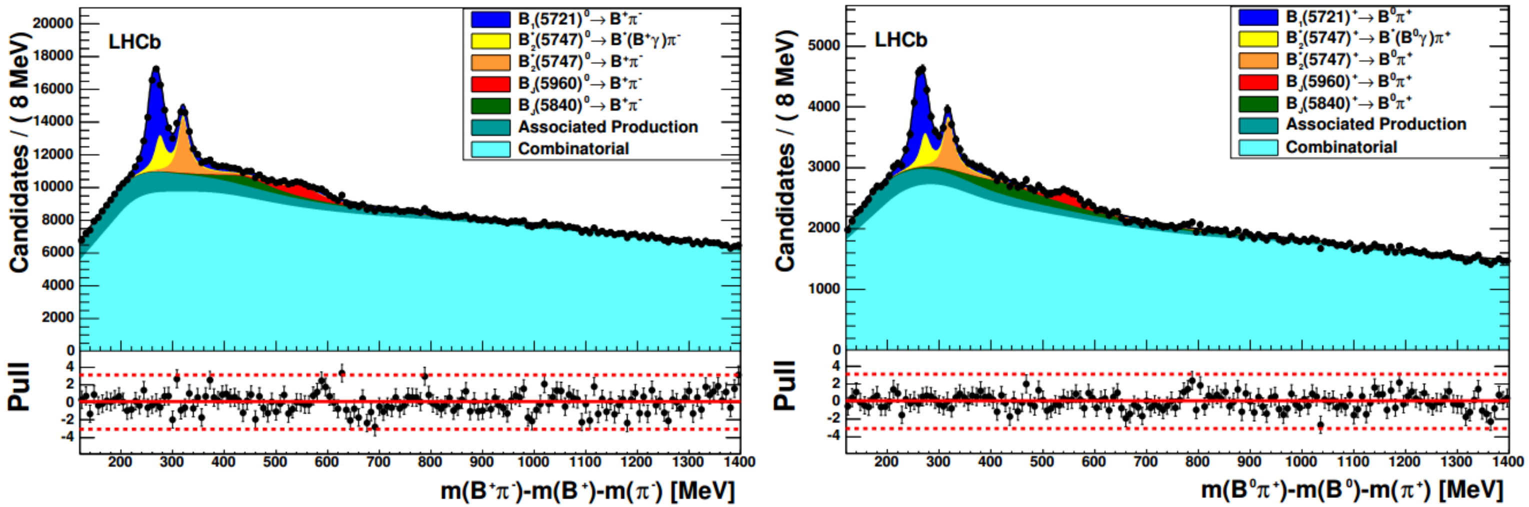

- Resonances - Relativistic Breit-Wigner shape
  - Most natural spin-parity states can decay to both $B\pi$ and $B^*\pi$
  - Since $B^*\pi \to B\pi\gamma$, include two peaks for natural spin-parity states
- Combinatorial background - Shape from wrong sign decays in data (i.e. $B^+\pi^+$)
- Associated production - Fitted with empirical model from simulation
  - From very broad resonances or non-resonant production of B and π

$B^+\pi^-$ candidate fit in p_T bins

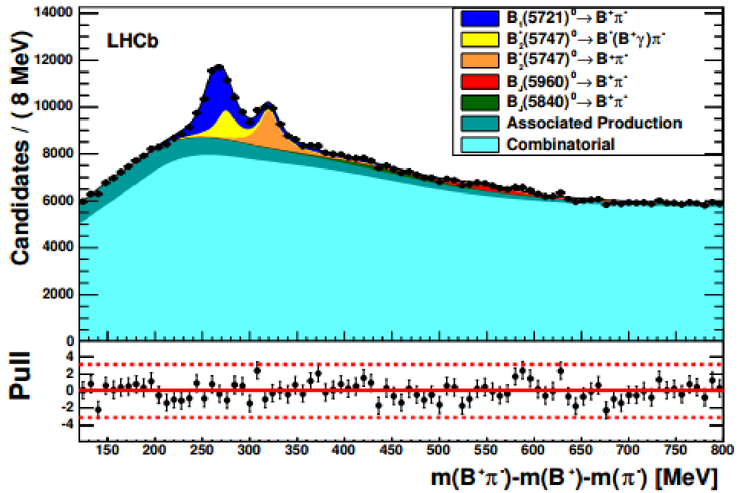

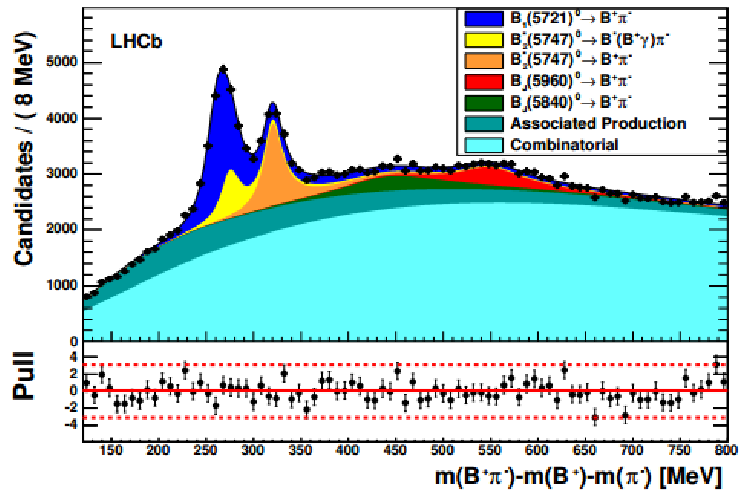

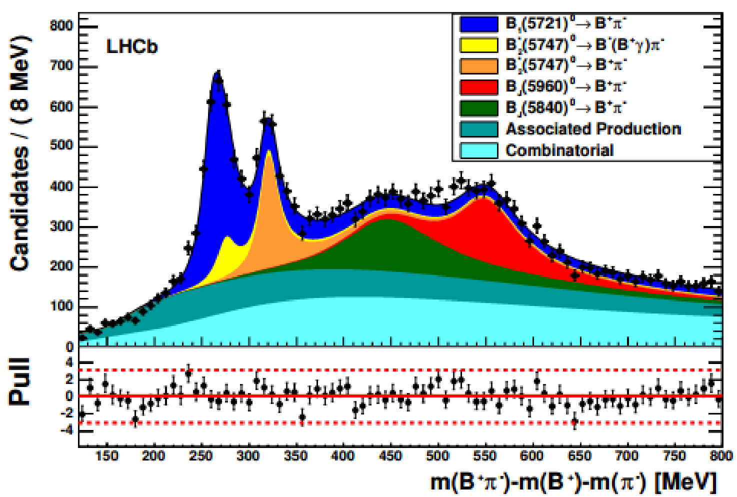

Data binned in p_T of π^-

- (top left) $0.5 < p_T < 1$ GeV
- (top left) $1 < p_T < 2$ GeV
- (bottom) $p_T > 2$ GeV

Similar plots for $B^0\pi^+$ in backup

Two RBWs used to fit high mass structure – alternative models with 3 RBWs

THE UNIVERSITY OF WARWICK

LHCb

Results

- Mass and width measurements presented for narrow states
  - Measurements agree with (but are more precise than) CDF results

$m_{B_1(5721)^0}$	$=$	5727.7	$\pm$	0.7	$\pm$	1.4	$\pm$	0.17	$\pm$	0.4	MeV
$m_{B_2^*(5747)^0}$	$=$	5739.44	$\pm$	0.37	$\pm$	0.33	$\pm$	0.17			MeV
$m_{B_1(5721)^+}$	$=$	5725.1	$\pm$	1.8	$\pm$	3.1	$\pm$	0.17	$\pm$	0.4	MeV
$m_{B_2^*(5747)^+}$	$=$	5737.20	$\pm$	0.72	$\pm$	0.40	$\pm$	0.17			MeV
$\Gamma_{B_1(5721)^0}$	$=$	30.1	$\pm$	1.5	$\pm$	3.5					MeV
$\Gamma_{B_2^*(5747)^0}$	$=$	24.5	$\pm$	1.0	$\pm$	1.5					MeV
$\Gamma_{B_1(5721)^+}$	$=$	29.1	$\pm$	3.6	$\pm$	4.3					MeV
$\Gamma_{B_2^*(5747)^+}$	$=$	23.6	$\pm$	2.0	$\pm$	2.1					MeV

(Uncertainties are stat., syst., uncertainty on B meson mass, uncertainty on $B^* - B$ mass difference)

- Branching fraction ratios measured for B_2^* states – in agreement with theory predictions
  - First evidence of $B_2^*(5747)^0 \to B^{*+}\pi^-$ decay

$$\frac{\mathcal{B}\left(B_2^*(5747)^0 \to B^{*+}\pi^-\right)}{\mathcal{B}\left(B_2^*(5747)^0 \to B^{+}\pi^-\right)} = 0.71 \pm 0.14 \pm 0.30$$

$$\frac{\mathcal{B}\left(B_2^*(5747)^+ \to B^{*0}\pi^+\right)}{\mathcal{B}\left(B_2^*(5747)^+ \to B^{0}\pi^+\right)} = 1.0 \pm 0.5 \pm 0.8$$

[Phys. Rev. D86 (2012) 054024, Eur. Phys. J. C9 (1999) 503, Phys. Rev. D58 (1998) 074009, Phys. Rev. D78 (2008) 014029, Phys. Rev. D43 (1991) 1679]

(Uncertainties are statistical and systematic)

- Structure at high mass clearly observed; measured parameters and interpretation depend on model assumptions

Conclusions

- Several spectroscopy results produced from LHCb in the last few months
  - Observation of Ξ_b^- resonances [Phys. Rev. Lett. 114 (2015) 062004]
  - Dalitz plot analysis $B_s^0 \to \overline{D}^0 K^- \pi^+$ [Phys. Rev. D90 (2014) 072003, Phys. Rev. Lett. 113 (2014) 162001]

- New D^{**} results from Dalitz plot analysis of $B^- \to D^+ K^- \pi^-$ decays
  - First observation of $B^- \to D^+ K^- \pi^-$ decay
  - $D_1^*(2760)^0$ determined to have spin-1
  - Masses and widths of $D_2^*(2460)^0$ and $D_1^*(2760)^0$ measured
  - Product branching fractions of resonances measured

- New B^{**} results from studies of $B^0\pi^+$ and $B^+\pi^-$ mass distributions
  - First evidence of $B_2^*(5747)^0 \to B^{*+}\pi^-$ decay
  - Masses and widths of $B_1(5721)$ and $B_2^*(5747)$ states measured
  - Results for higher mass states depend on fit model used

- Look out for studies of additional modes coming soon!

Backup

LHCb overview

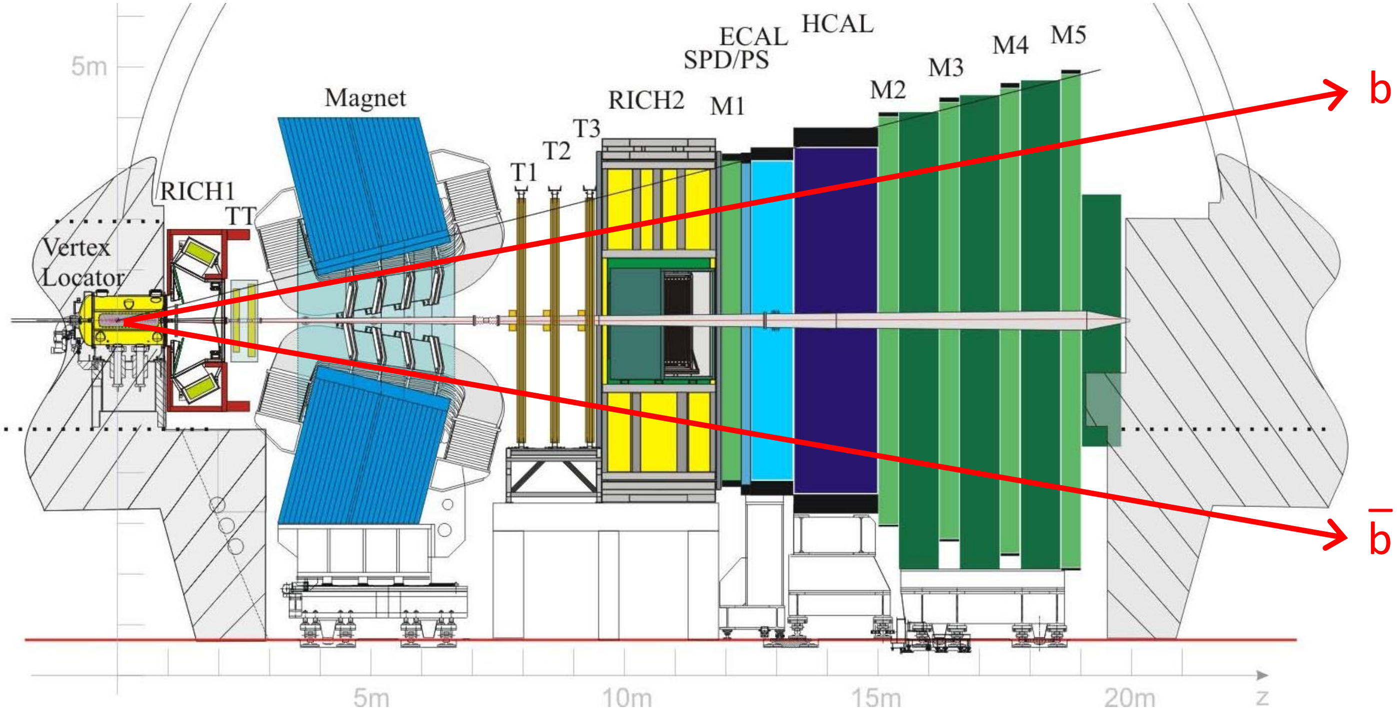

- Long lived heavy hadrons are predominantly produced in the forward direction
- LHCb geometry exploits this fact

- Vertex Locator (VELO) – precise tracking very close to the interaction point
- Two Ring Imaging Cherenkov (RICH) detectors – separation of kaons and pions

Trigger categories at LHCb

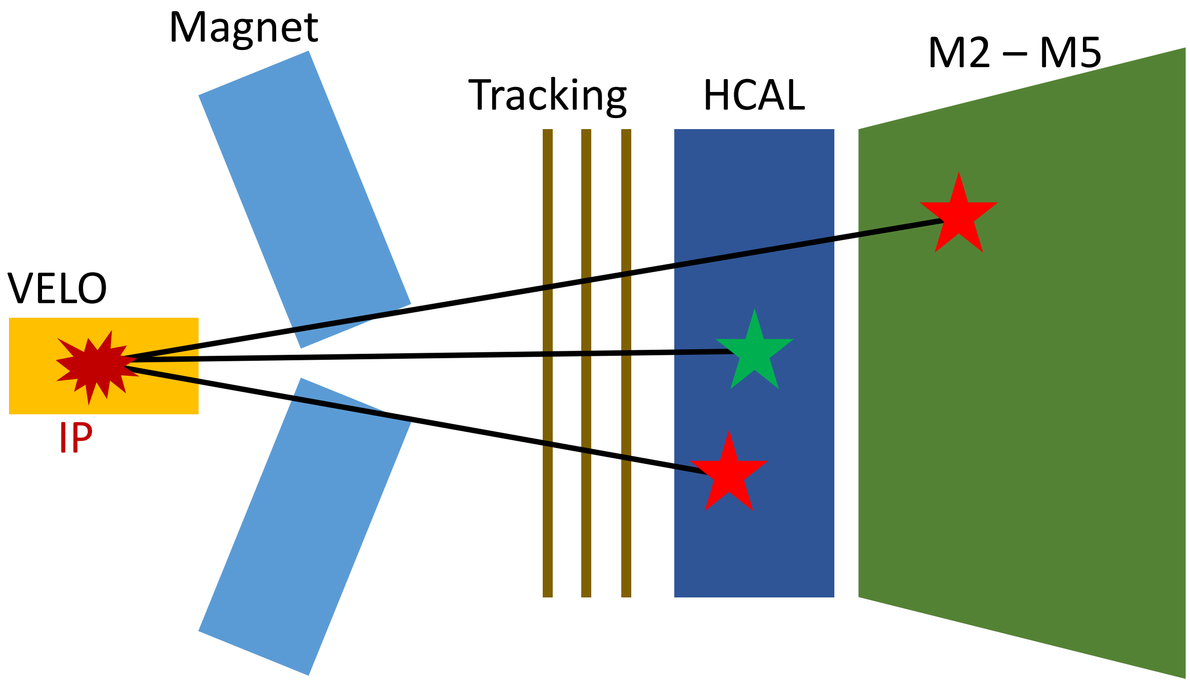

- Trigger On Signal – particle from signal decay fires trigger
  - HCAL deposits

- Trigger Independent of Signal – particle from rest of the event fires trigger
  - HCAL deposits and muon hits

Square Dalitz plot

- Coordinate transform of Dalitz plot to give a square phase space
- In this choice of SDP representation, m' is related to $m(D\pi)$ in reverse and θ' is the $D\pi$ helicity angle
  - Resonances decaying to $D^+\pi^-$ appear vertically at high m'

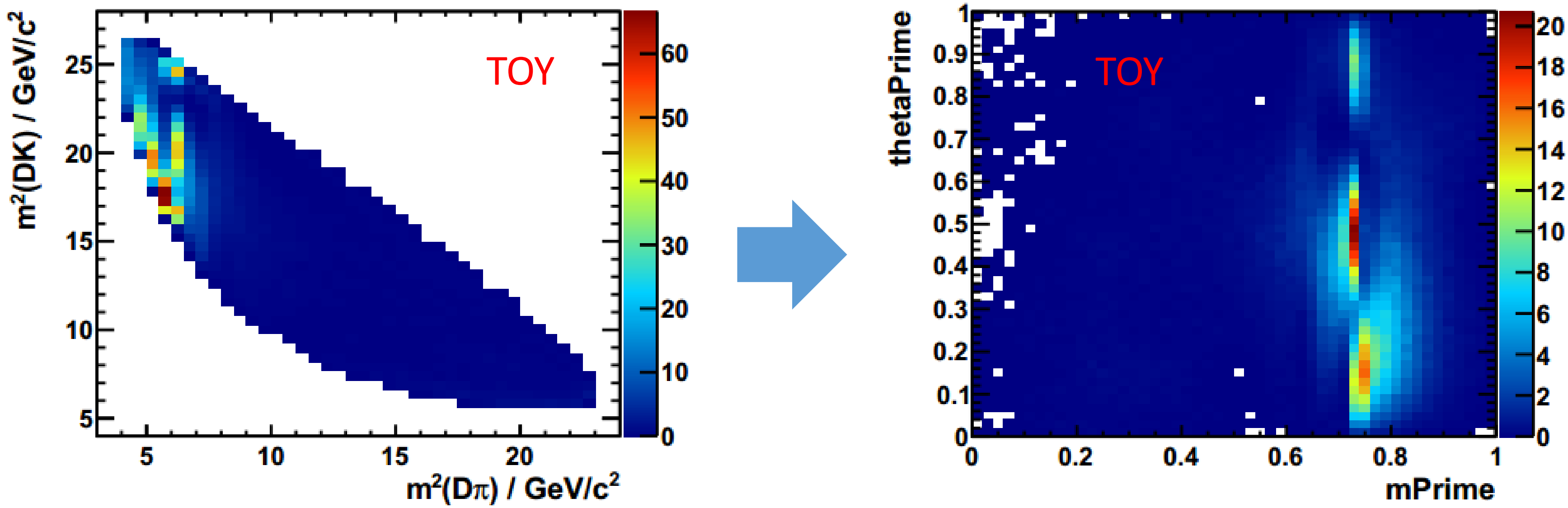

$B^- \to D^+ K^- \pi^-$ branching fraction

- Systematics evaluated:

Source	Uncertainty (%)
Λ_c^+ veto	0.2
Fit model	2.0
Particle identification	2.1
Efficiency modelling	0.8
Total	3.0

- BF measured w.r.t. topologically similar $B^- \to D^+ \pi^- \pi^-$

$$\frac{\mathcal{B}(B^- \to D^+ K^- \pi^-)}{\mathcal{B}(B^- \to D^+ \pi^- \pi^-)} = 0.0702 \pm 0.0020 \pm 0.0021$$

$$\boxed{\mathcal{B}(B^- \to D^+ K^- \pi^-) = (7.92 \pm 0.23 \pm 0.24 \pm 0.42) \times 10^{-5}}$$

Uncertainties are statistical, systematic and due to PDG uncertainty on $B^- \to D^+ \pi^- \pi^-$ BF

$B^- \rightarrow D^+K^-\pi^-$ selection

- Identical selection applied to $D\pi\pi$ and $DK\pi$ candidates apart from Particle Identification (PID) requirement on the one different track.

- D candidates reconstructed as $D^+ \rightarrow K^-\pi^+\pi^+$

- Loose initial requirements applied to suppress background contributions

- $D\pi\pi$ data used to train two neural netowrks – first to clean up D candidates, second to suppress combinatorial background
  - sPlot technique used to statistically separate signal and background events
  - Combinatorial background reduced by an order of magnitude, 90% signal kept

- PID requirements applied to all 5 final state tracks

Backgrounds

- Signal region is taken as $\pm 2.5\sigma$

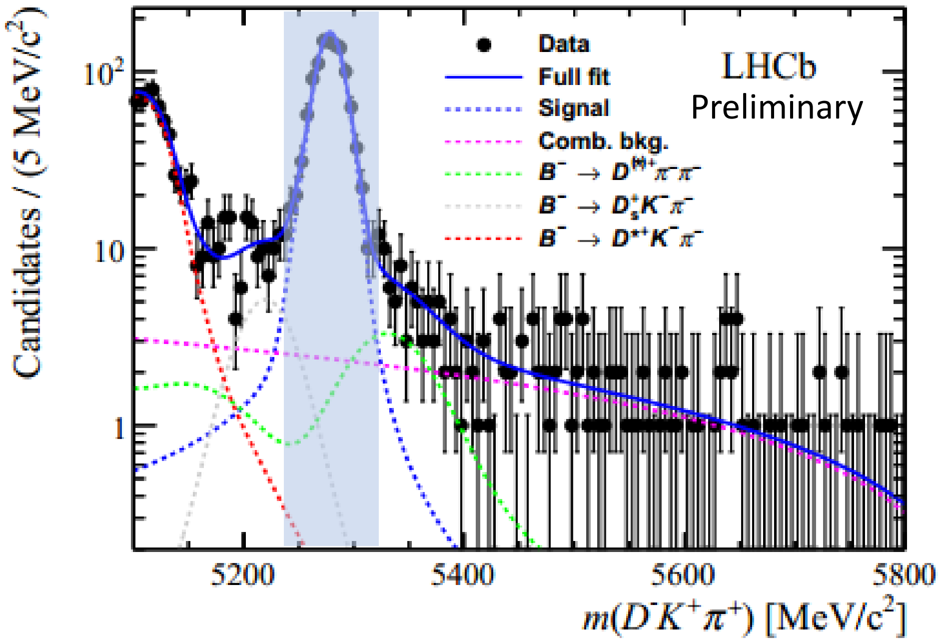

- Signal region is 93.2% pure – three backgrounds contribute: $B^- \to D_s^+ K^- \pi^-$ (1.4%), $B^- \to D^+ \pi^- \pi^-$ (1.7%), combinatorial (3.5%)

Efficiency and background distributions

- Signal efficiency distribution for events triggered by (left) particles in the candidate decay, (right) other particles in the event

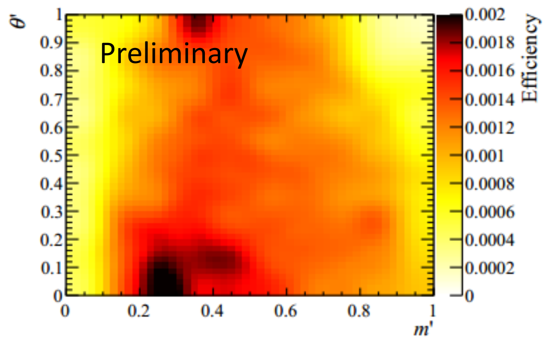

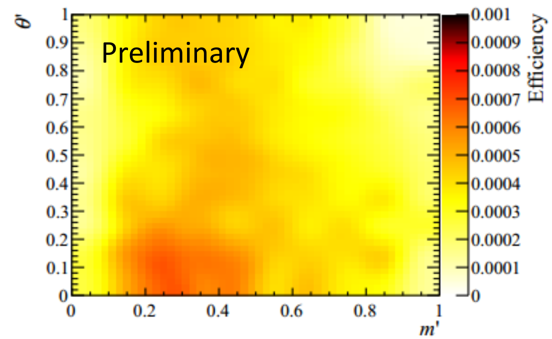

- Signal region is 93% pure – three backgrounds contribute: (left) $B^- \rightarrow D_s^+ K^- \pi^-$, (middle) $B^- \rightarrow D^+ \pi^- \pi^-$, (right) combinatorial

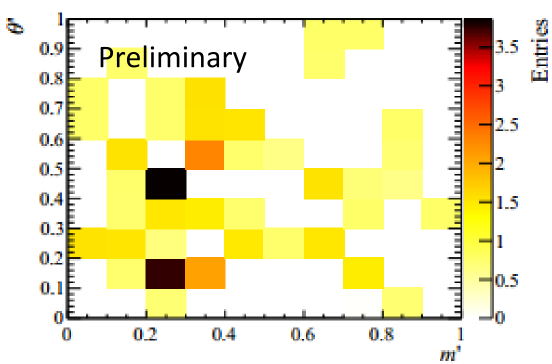

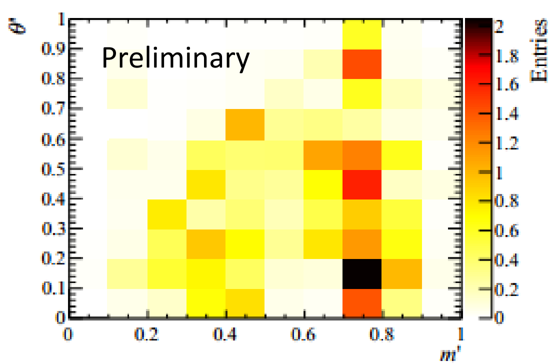

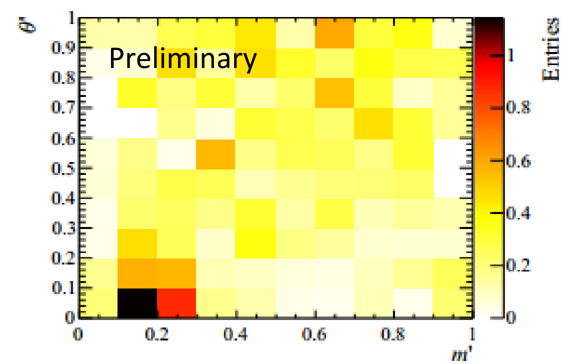

Previous D^{**} spectroscopy measurements

Resonance	Mass (MeV/c^2)	Width (MeV)	J^P	
$D_0^*(2400)^0$	2318 ± 29	267 ± 40	0^+	[1]
$D_1(2420)^0$	2421.4 ± 0.6	27.4 ± 2.5	1^+	[1]
$D_1'(2430)^0$	$2427 \pm 26 \pm 20 \pm 15$	$384\,^{+107}_{-75} \pm 24 \pm 70$	1^+	[2]
$D_2^*(2460)^0$	2462.6 ± 0.6	49.0 ± 1.3	2^+	[1]
$D^*(2600)$	$2608.7 \pm 2.4 \pm 2.5$	$93 \pm 6 \pm 13$	natural	[3]
$D^*(2650)$	$2649.2 \pm 3.5 \pm 3.5$	$140 \pm 17 \pm 19$	natural	[4]
$D^*(2760)$	$2763.3 \pm 2.3 \pm 2.3$	$60.9 \pm 5.1 \pm 3.6$	natural	[3]
$D^*(2760)$	$2760.1 \pm 1.1 \pm 3.7$	$74.4 \pm 3.4 \pm 19.1$	natural	[4]

[1] Chin. Phys. C, 38, 090001 (2014)
[2] Phys.Rev. D69 (2004) 112002
[3] Phys.Rev. D82 (2010) 111101
[4] JHEP 1309 (2013) 145

Fit results

Resonance	Real part	Imaginary part	Magnitude	Phase
	Isobar model coefficients			
$D_0^*(2400)^0$	$-0.04 \pm 0.07 \pm 0.03 \pm 0.28$	$-0.51 \pm 0.07 \pm 0.02 \pm 0.13$	$0.51 \pm 0.09 \pm 0.02 \pm 0.15$	$-1.65 \pm 0.16 \pm 0.06 \pm 0.50$
$D_2^*(2460)^0$	1.00	0.00	0.00	0.00
$D_1^*(2760)^0$	$-0.32 \pm 0.06 \pm 0.03 \pm 0.03$	$-0.23 \pm 0.07 \pm 0.03 \pm 0.03$	$0.39 \pm 0.05 \pm 0.01 \pm 0.03$	$-2.53 \pm 0.24 \pm 0.08 \pm 0.08$
Nonresonant (S-wave)	$0.93 \pm 0.09 \pm 0.03 \pm 0.17$	$-0.58 \pm 0.08 \pm 0.03 \pm 0.15$	$1.09 \pm 0.09 \pm 0.02 \pm 0.20$	$-0.56 \pm 0.09 \pm 0.04 \pm 0.11$
Nonresonant (P-wave)	$-0.43 \pm 0.09 \pm 0.03 \pm 0.34$	$0.75 \pm 0.09 \pm 0.05 \pm 0.68$	$0.87 \pm 0.09 \pm 0.03 \pm 0.11$	$2.09 \pm 0.15 \pm 0.05 \pm 0.95$
$D_v^*(2007)^0$	$0.16 \pm 0.08 \pm 0.03 \pm 0.56$	$0.46 \pm 0.09 \pm 0.04 \pm 0.77$	$0.49 \pm 0.07 \pm 0.04 \pm 0.05$	$1.24 \pm 0.17 \pm 0.07 \pm 0.60$
B_v^*	$-0.07 \pm 0.08 \pm 0.22 \pm 0.09$	$0.33 \pm 0.07 \pm 0.02 \pm 0.08$	$0.34 \pm 0.06 \pm 0.03 \pm 0.07$	$1.78 \pm 0.23 \pm 0.11 \pm 0.27$

Resonance	Fit fraction
$D_0^*(2400)^0$	$8.3 \pm 2.6 \pm 0.6 \pm 1.9$
$D_2^*(2460)^0$	$31.8 \pm 1.5 \pm 0.9 \pm 1.4$
$D_1^*(2760)^0$	$4.9 \pm 1.2 \pm 0.3 \pm 0.9$
Nonresonant (S-wave)	$38.0 \pm 7.4 \pm 1.5 \pm 10.8$
Nonresonant (P-wave)	$23.8 \pm 5.6 \pm 2.1 \pm 3.7$
$D_v^*(2007)^0$	$7.6 \pm 2.3 \pm 1.3 \pm 1.5$
B_v^*	$3.6 \pm 1.9 \pm 0.9 \pm 1.6$

Parameter	Value
α_S	0.36 ± 0.03
α_P	0.36 ± 0.04

Legendre moments for $B^- \to D^+K^-\pi^-$

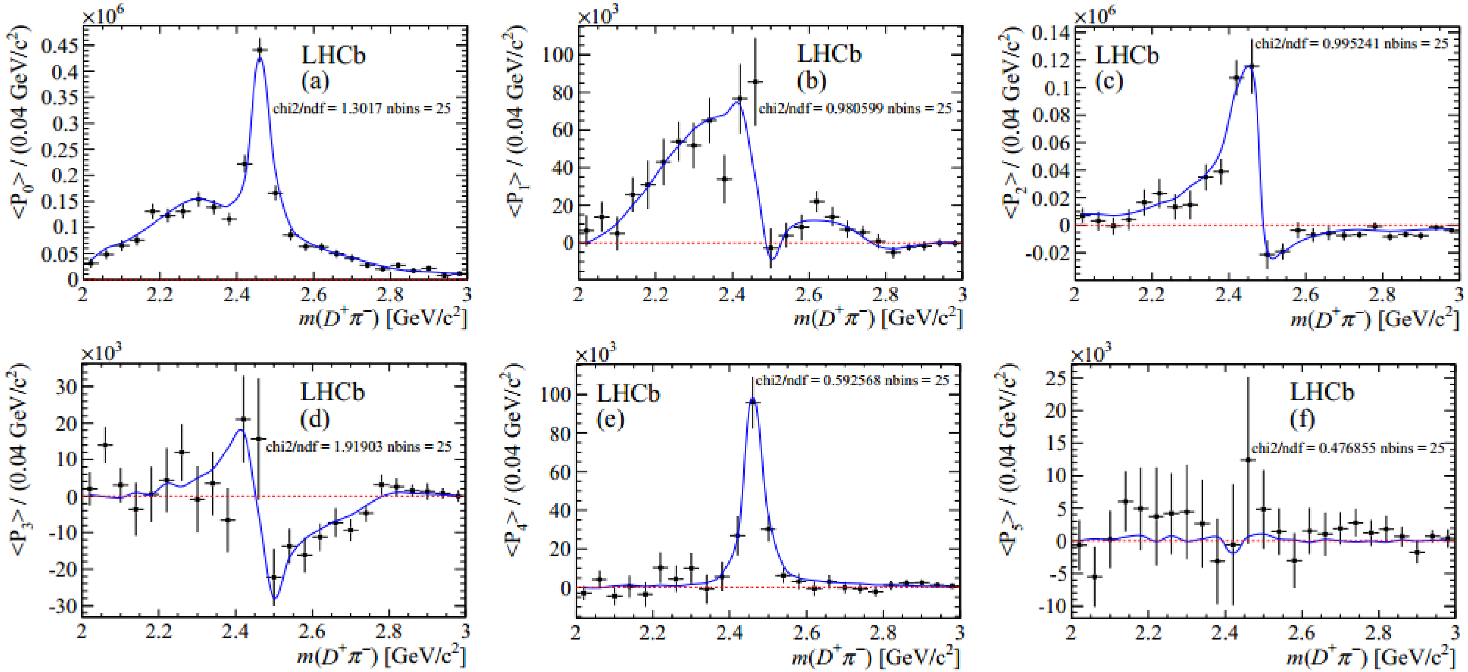

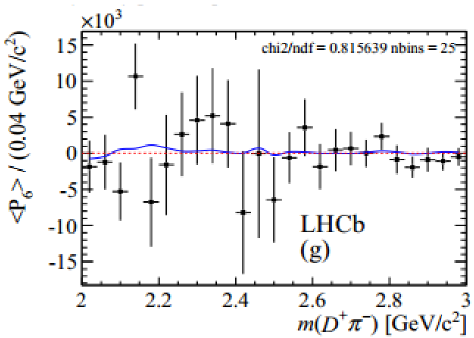

- Moments for $m(D\pi)$
- **Data** and **fit model**
- No structure in P_5 and P_6 suggest <u>no spin-3</u> contribution in data

Goodness of fit for $B^- \to D^+ K^- \pi^-$ Dalitz plot fit

- Adaptive binning – equal number of events per bin
- 1.38 < χ^2/ndf < 1.68
  - ndf between nbins-1 and nbins-npars-1
- Fits to toy data support result of χ^2/ndf = 1.68 for binning choice
- Pulls across SDP shown:

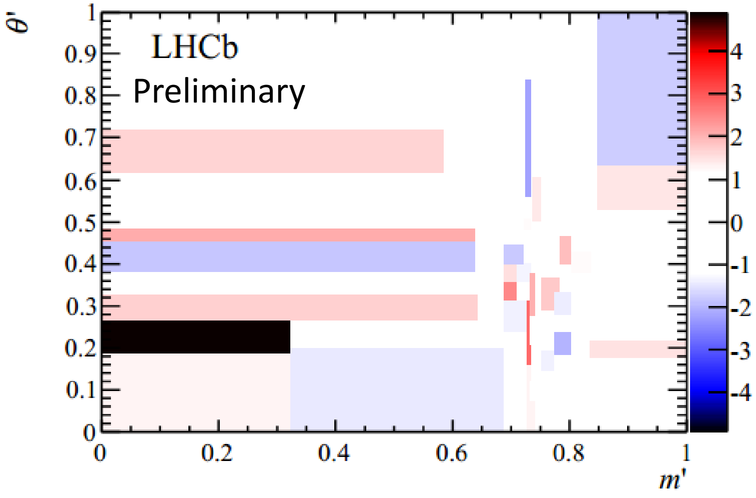

$B^- \to D^+ K^- \pi^-$ DP systematics

- Extensive systematic studies performed
  - Systematic uncertainties calculated for all reported fit parameters
  - All systematics have varying effects on measured quantities but systematics that tend to dominate are shown in red

- Experimental systematics
  - Signal and background yields
  - Efficiency distribution
  - Background distributions
  - Fit bias

- Model uncertainties
  - Fixed parameters in DP model
  - Test model (add/remove marginal components)
  - Alternative models for non-resonant and virtual components

$B^0\pi^+$ candidate fit in p_T bins

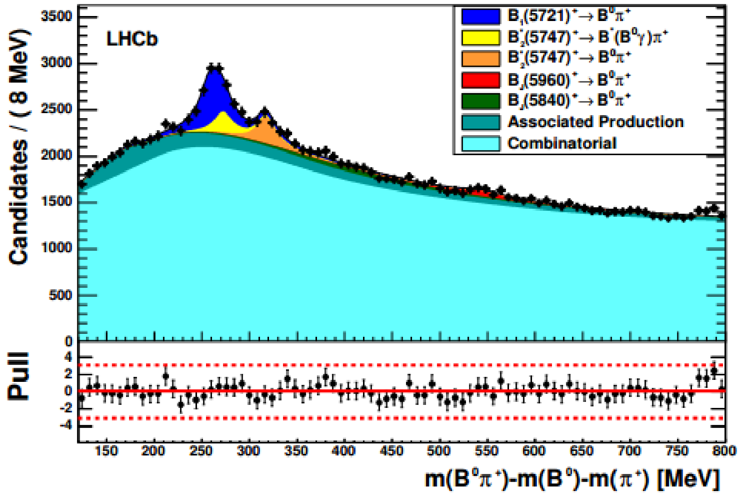

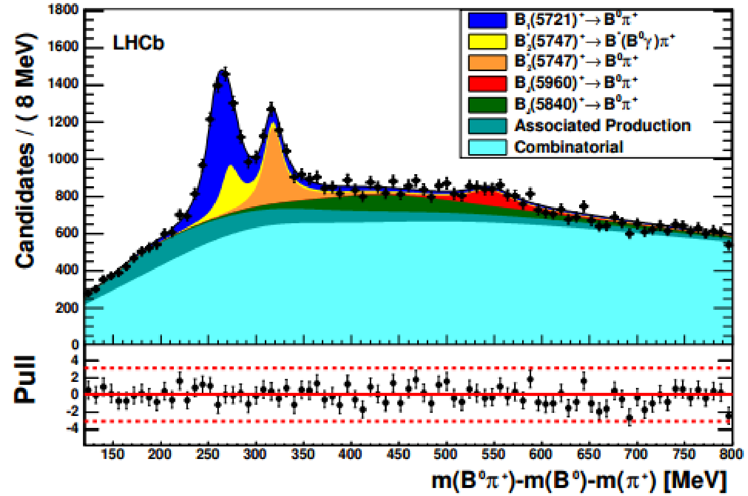

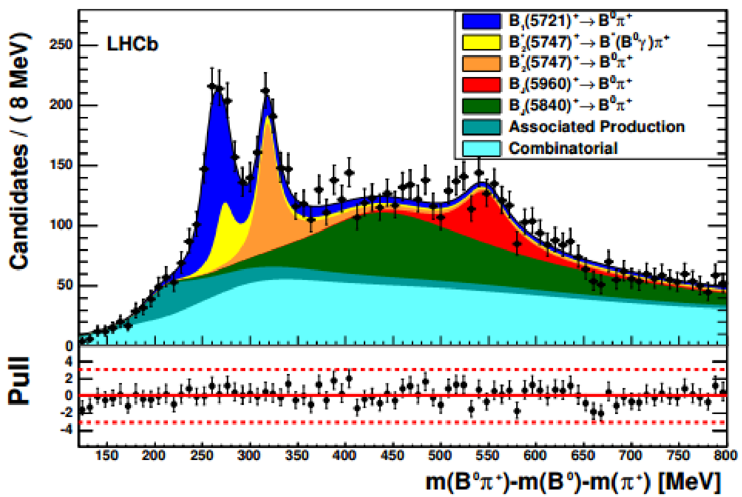

Fit $Q = m(B\pi) - m_B - m_\pi$ for $B^0\pi^+$

Data binned in p_T of π^+
- (top left) $0.5 < p_T < 1$ GeV
- (top left) $1 < p_T < 2$ GeV
- (bottom) $p_T > 2$ GeV

THE UNIVERSITY OF WARWICK

Fit results (stat. uncertainties only)

Fit parameter	$B^+\pi^-$	$B^0\pi^+$
$B_1(5721)^{0,+}$ μ	263.9 ± 0.7	260.9 ± 1.8
$B_1(5721)^{0,+}$ Γ	30.1 ± 1.5	29.1 ± 3.6
$B_2^*(5747)^{0,+}$ μ	320.6 ± 0.4	318.1 ± 0.7
$B_2^*(5747)^{0,+}$ Γ	24.5 ± 1.0	23.6 ± 2.0
$N_{B_1(5721)^{0,+}}$ low p_T	14200 ± 1400	3140 ± 750
$N_{B_1(5721)^{0,+}}$ mid p_T	16200 ± 1500	4020 ± 890
$N_{B_1(5721)^{0,+}}$ high p_T	4830 ± 470	940 ± 260
$N_{B_2^*(5747)^{0,+}}$ low p_T	7450 ± 420	1310 ± 180
$N_{B_2^*(5747)^{0,+}}$ mid p_T	7600 ± 340	2070 ± 180
$N_{B_2^*(5747)^{0,+}}$ high p_T	1690 ± 130	640 ± 80
$\mathcal{B}(B_2^*(5747)^{0,+} \to B^*\pi)/\mathcal{B}(B_2^*(5747)^{0,+} \to B\pi)$	0.71 ± 0.14	1.0 ± 0.5
$B_J(5840)^{0,+}$ μ	444 ± 5	431 ± 13
$B_J(5840)^{0,+}$ Γ	127 ± 17	224 ± 24
$B_J(5960)^{0,+}$ μ	550.4 ± 2.9	545.8 ± 4.1
$B_J(5960)^{0,+}$ Γ	82 ± 8	63 ± 15
$N_{B_J(5840)^{0,+}}$ low p_T	3200 ± 1300	1630 ± 970
$N_{B_J(5840)^{0,+}}$ mid p_T	5600 ± 1000	3230 ± 720
$N_{B_J(5840)^{0,+}}$ high p_T	3090 ± 550	2280 ± 450
$N_{B_J(5960)^{0,+}}$ low p_T	3270 ± 660	610 ± 240
$N_{B_J(5960)^{0,+}}$ mid p_T	4590 ± 610	910 ± 250
$N_{B_J(5960)^{0,+}}$ high p_T	2400 ± 320	500 ± 140

Parameters for high mass states

(Uncertainties are statistical, experimental systematic, uncertainty on B meson mass, uncertainty on $B^{*} - B$ mass difference)

Any state not labelled "natural" is assumed to have unnatural spin-parity

	Empirical model
$m_{B_J(5840)^0}$	$5862.9 \pm 5.0 \pm 6.7 \pm 0.2$
$\Gamma_{B_J(5840)^0}$	$127.4 \pm 16.7 \pm 34.2$
$m_{B_J(5960)^0}$	$5969.2 \pm 2.9 \pm 5.1 \pm 0.2$
$\Gamma_{B_J(5960)^0}$	$82.3 \pm 7.7 \pm 9.4$
$m_{B_J(5840)^+}$	$5850.3 \pm 12.7 \pm 13.7 \pm 0.2$
$\Gamma_{B_J(5840)^+}$	$224.4 \pm 23.9 \pm 79.8$
$m_{B_J(5960)^+}$	$5964.9 \pm 4.1 \pm 2.5 \pm 0.2$
$\Gamma_{B_J(5960)^+}$	$63.0 \pm 14.5 \pm 17.2$
	Quark model, $B_J(5840)^{0,+}$ natural
$m_{B_J(5840)^0}$	$5889.7 \pm 22.2 \pm 6.7 \pm 0.2$
$\Gamma_{B_J(5840)^0}$	$107.0 \pm 19.6 \pm 34.2$
$m_{B_J(5960)^0}$	$6015.9 \pm 3.7 \pm 5.1 \pm 0.2 \pm 0.4$
$\Gamma_{B_J(5960)^0}$	$81.6 \pm 9.9 \pm 9.4$
$m_{B_J(5840)^+}$	$5874.5 \pm 25.7 \pm 13.7 \pm 0.2$
$\Gamma_{B_J(5840)^+}$	$214.6 \pm 26.7 \pm 79.8$
$m_{B_J(5960)^+}$	$6010.6 \pm 4.0 \pm 2.5 \pm 0.2 \pm 0.4$
$\Gamma_{B_J(5960)^+}$	$61.4 \pm 14.5 \pm 17.2$
	Quark model, $B_J(5960)^{0,+}$ natural
$m_{B_J(5840)^0}$	$5907.8 \pm 4.7 \pm 6.7 \pm 0.2 \pm 0.4$
$\Gamma_{B_J(5840)^0}$	$119.4 \pm 17.2 \pm 34.2$
$m_{B_J(5960)^0}$	$5993.6 \pm 6.4 \pm 5.1 \pm 0.2$
$\Gamma_{B_J(5960)^0}$	$55.9 \pm 6.6 \pm 9.4$
$m_{B_J(5840)^+}$	$5889.3 \pm 15.0 \pm 13.7 \pm 0.2 \pm 0.4$
$\Gamma_{B_J(5840)^+}$	$229.3 \pm 26.9 \pm 79.8$
$m_{B_J(5960)^+}$	$5966.4 \pm 4.5 \pm 2.5 \pm 0.2$
$\Gamma_{B_J(5960)^+}$	$60.8 \pm 14.0 \pm 17.2$